Annals of Botany **111**: 577–589, 2013
doi:10.1093/aob/mct017, available online at www.aob.oxfordjournals.org

ANNALS OF BOTANY
Founded 1887

Significant involvement of PEP-CK in carbon assimilation of C_4 eudicots

Riyadh Muhaidat[1] and Athena D. McKown[2,*]

[1]*Department of Biological Sciences, Faculty of Science, Yarmouk University, Irbid, PO 21163, Hashemite Kingdom of Jordan and* [2]*Department of Forest and Conservation Sciences, Faculty of Forestry, University of British Columbia, Forest Sciences Centre, 2424 Main Mall, Vancouver, BC V6T 1Z4, Canada*
** For correspondence. E-mail admckown@gmail.com*

Received: 18 October 2012 Revision requested: 16 November 2012 Accepted: 17 December 2012 Published electronically: 6 February 2013

• *Background and Aims* C_4 eudicot species are classified into biochemical sub-types of C_4 photosynthesis based on the principal decarboxylating enzyme. Two sub-types are known, NADP-malic enzyme (ME) and NAD-ME; however, evidence for the occurrence or involvement of the third sub-type (phospho*enol*pyruvate carboxykinase; PEP-CK) is emerging. In this study, the presence and activity of PEP-CK in C_4 eudicot species of *Trianthema* and *Zaleya* (Sesuvioideae, Aizoaceae) is clarified through analysis of key anatomical features and C_4 photosynthetic enzymes.
• *Methods* Three C_4 species (*T. portulacastrum*, *T. sheilae* and *Z. pentandra*) were examined with light and transmission electron microscopy for leaf structural properties. Activities and immunolocalizations of C_4 enzymes were measured for biochemical characteristics.
• *Key Results* Leaves of each species possess atriplicoid-type *Kranz* anatomy, but differ in ultrastructural features. Bundle sheath organelles are centripetal in *T. portulacastrum* and *Z. pentandra*, and centrifugal in *T. sheilae*. Bundle sheath chloroplasts in *T. portulacastrum* are almost agranal, whereas mesophyll counterparts have grana. Both *T. sheilae* and *Z. pentandra* are similar, where bundle sheath chloroplasts contain well-developed grana while mesophyll chloroplasts are grana deficient. Cell wall thickness is significantly greater in *T. sheilae* than in the other species. Biochemically, *T. portulacastrum* is NADP-ME, while *T. sheilae* and *Z. pentandra* are NAD-ME. Both *T. portulacastrum* and *Z. pentandra* exhibit considerable PEP-CK activity, and immunolocalization studies show dense and specific compartmentation of PEP-CK in these species, consistent with high PEP-CK enzyme activity.
• *Conclusions* Involvement of PEP-CK in C_4 NADP-ME *T. portulacastrum* and NAD-ME *Z. petandra* occurs irrespective of biochemical sub-type, or the position of bundle sheath chloroplasts. Ultrastructural traits, including numbers of bundle sheath peroxisomes and mesophyll chloroplasts, and degree of grana development in bundle sheath chloroplasts, coincide more directly with PEP-CK recruitment. Discovery of high PEP-CK activity in C_4 Sesuvioideae species offers a unique opportunity for evaluating PEP-CK expression and suggests the possibility that PEP-CK recruitment may exist elsewhere in C_4 eudicots.

Key words: Aizoaceae, C_4 photosynthesis, granal development, *Kranz* anatomy, NADP-ME sub-type, NAD-ME sub-type, PEP-CK sub-type, Sesuvioideae, thylakoid, *Trianthema portulacastrum*, *Trianthema sheilae*, *Zaleya pentandra*.

INTRODUCTION

Carbon assimilation by the photosynthetic enzyme Rubisco (ribulose-1,5-bisphosphate carboxylase/oxygenase) is susceptible to inefficiencies, including an oxygenase activity leading to energy loss through photorespiration and slow turnover of the protein (Sage, 2002; Parry *et al.*, 2007). Plants using C_4 photosynthesis overcome these inefficiencies by concentrating CO_2 around Rubisco sites to levels inhibiting the oxygenase activity and associated photorespiration (Kanai and Edwards, 1999). This is achieved in the majority of C_4 plants by splitting carbon assimilatory reactions between two distinct cell types, bundle sheath (BS) and mesophyll (M), and arranging these tissues in particular patterns termed *Kranz* anatomy (Dengler and Nelson, 1999; Edwards and Voznesenskaya, 2011). The carbon reactions are generally separated into: (1) photosynthetic carbon assimilation reactions involving enzymes that incorporate CO_2 into C_4 acids (malate/aspartate); and (ii) photosynthetic carbon reduction reactions involving enzymes for decarboxylating C_4 acids to release CO_2, and for the C_3 cycle. In C_4 plants, assimilation and C_4 acid-forming enzymes, such as phospho*enol*pyruvate-carboxylase (PEPC) and pyruvate-orthophosphate dikinase (PPdK), are localized in M cells, whereas decarboxylation enzymes, Rubisco and the C_3 cycle are restricted to BS cells (Kanai and Edwards, 1999).

Many anatomical and biochemical forms of C_4 photosynthesis exist among C_4 plants, and phylogenetic reconstructions support their independent origins during the evolutionary course of angiosperms (Dengler and Nelson, 1999; Sage, 2004; Muhaidat *et al.*, 2007). Regardless of evolutionary heritage, C_4 plants are categorized into biochemical sub-types based on the predominant enzyme used for C_4 acid decarboxylation in BS cells: NADP-malic enzyme (NADP-ME), NAD-malic enzyme (NAD-ME) and phospho*enol*pyruvate carboxykinase (PEP-CK) sub-types (Kanai and Edwards, 1999; see Furbank, 2011 for a different opinion). The three

sub-types are found throughout the grasses (Poaceae), whereas only the NADP-ME and NAD-ME sub-types have been found in 16 eudicot families with C_4 photosynthesis (Muhaidat *et al.*, 2007; Sage *et al.*, 2011). Surveys in Poaceae and most eudicot families show robust correspondence between C_4 biochemical sub-type and BS ultrastructural features (reviewed in Dengler and Nelson, 1999). For instance, BS cells in NADP-ME C_4 species possess chloroplasts with reduced granal development (i.e. lower thylakoid stacking) and few, small mitochondria, while BS cells in NAD-ME and PEP-CK (grasses) C_4 species have granal chloroplasts (i.e. higher thylakoid stacking) and numerous, large mitochondria (Gutierrez *et al.*, 1974; Hatch *et al.*, 1975; Hatch, 1987; Dengler and Nelson, 1999; Yoshimura *et al.*, 2004; Edwards and Voznesenskaya, 2011).

The PEP-CK biochemical sub-type is not known to have evolved in C_4 eudicots, and is a central question that remains enigmatic (Furbank, 2011). Since early explorations of C_4 photosynthesis, it has been concluded that a PEP-CK type C_4 cycle is not likely in C_4 eudicots based on very low or undetectable PEP-CK activities in a limited number of C_4 eudicot species studied (Gutierrez *et al.*, 1974; Hatch *et al.*, 1975; Ku *et al.*, 1983). The assumption that the PEP-CK sub-type is non-existent in extant C_4 eudicots, however, may be debatable. Recent evidence in support of PEP-CK recruitment was described in large anatomical and biochemical surveys of C_4 eudicots (Marshall *et al.*, 2007; Muhaidat *et al.*, 2007; Sommer *et al.*, 2012). Muhaidat *et al.* (2007) recorded high PEP-CK levels in certain C_4 eudicot species in the Aizoaceae (NADP-ME *Trianthema portulacastrum* and NAD-ME *Zaleya pentandra*) and Nyctaginaceae (NADP-ME *Boerhavia domnii* and *B. coccinea*). The reported values were in the range characteristic of PEP-CK C_4 grasses (Gutierrez *et al.*, 1974; Hatch *et al.*, 1975; Prendergast *et al.*, 1987). Moreover, immunolocalization studies comparing PEP-CK *Melinis minutiflora* (Poaceae) and NAD-ME *Cleome gynandra* (Cleomaceae) revealed strong localization of the PEP-CK enzyme specifically in the BS tissue of *C. gynandra* (R. Muhaidat and J. M. Hibberd, unpubl. res.). Further work in *C. gynandra* showed selective accumulation of PEP-CK transcripts in BS cells, and considerable engagement of the PEP-CK pathway alongside the NAD-ME pathway in mature leaves (Marshall *et al.*, 2007; Sommer *et al.*, 2012).

Two of the putative 'PEP-CK'-like C_4 eudicot species (*T. portulacastrum* and *Z. pentandra*) are in the ice plant family Aizoaceae (Muhaidat *et al.*, 2007). Aizoaceae is a cosmopolitan and strikingly diverse family (Hartmann, 2001*a*, *b*). Members are predominantly succulent herbs and small shrubs widely distributed in arid, semi-arid and saline habitats of the tropics and sub-tropics, with the highest species frequency in the arid winter rainfall area of Southern Africa (Hartmann, 2001*a*, *b*; Klak *et al.*, 2003). Taxonomically, Aizoaceae is split into four subfamilies (Aizooideae, Sesuvioideae, Ruschioideae and Mesembryanthemoideae) based on four plastid DNA markers (Klak *et al.*, 2003). Among these subfamilies, only Sesuvioideae is known to contain genera with C_4 species based on screens of carbon isotopic composition ($\delta^{13}C$; Sage, 2004), including *Cypselea* Turp., *Sesuvium* L., *Trianthema* L. and *Zaleya* Burm.f. (Hassan *et al.*, 2005). Leaves of C_4 Sesuvioideae species studied thus far contain the 'atriplicoid-type' *Kranz* anatomy where BS and M cells form concentric tissue layers around vascular bundles (Muhaidat *et al.*, 2007). In comparison, BS organelles may differ between species in ultrastructure and placement, and may be centripetally (i.e. near the vasculature) or centrifugally positioned (i.e. away from the vasculature) (Carolin *et al.*, 1978; Muhaidat *et al.*, 2007). While both NADP-ME and NAD-ME biochemical sub-types are known in the Sesuvioideae, high PEP-CK activities and the varied ultrastructure and position of BS chloroplasts previously reported strongly suggest involvement of PEP-CK, warranting further investigation (Carolin *et al.*, 1978; Muhaidat *et al.*, 2007).

Using multiple lines of anatomical and biochemical evidence, we aimed to clarify and establish the presence or contribution of PEP-CK in C_4 eudicot species. In this study, we described key features from leaf anatomy and C_4 biochemistry, with specific reference to PEP-CK, in C_4 species of Sesuvioideae: *T. portulacastrum*, *T. sheilae* and *Z. pentandra*. To evaluate the presence of PEP-CK features, we assessed leaf anatomy by focusing specifically on placement and detailed ultrastructure of organelles in BS and M cells, and compared new enzyme activity data and enzyme localizations with previously published work by Muhaidat *et al.* (2007). Clarifying the presence or involvement of PEP-CK in carbon assimilation in multiple C_4 eudicots would suggest that this phenomenon is more diverse and widespread than previous assessments have indicated.

MATERIALS AND METHODS

Plant materials and growth conditions

A number of species were grown from seeds as study or comparison species (Table 1). Test species in the Aizoaceae [*Trianthema portulacastrum* L., *T. sheilae* A.G.Mill. & J.A.Nyberg and *Zaleya pentandra* (L.) C.Jeffrey] were grown from seeds collected from plants found in their natural habitats provided by R. Sage (University of Toronto, ON, Canada) and N. Kilian (Freie University, Berlin, Germany). Leaves of comparison species C_3 *Euphorbia peplus* L. (Euphorbiaceae) and C_4 NAD-ME *Amaranthus retroflexus* L. (Amaranthaceae) were collected from naturally growing plants at Yarmouk University (Irbid, Jordan). Seeds of comparison species C_4 NAD-ME *Cleome gynandra* L. were provided by R. Sage (University of Toronto, ON, Canada), and C_4 PEP-CK *Melinis minutiflora* P.Beauv. (Poaceae) by N. G. Dengler (University of Toronto, ON, Canada). Comparison species C_4 NADP-ME *Zea mays* L. (Poaceae) was grown from seeds purchased from local markets (Irbid, Jordan).

Anatomical, biochemical and immunological studies were all carried out on plants cultivated under greenhouse conditions at Yarmouk University (Irbid, Jordan). Seeds of all species were sown in 200 mL plastic pots filled with a soil mixture of 2:1:1 topsoil:sand:commercial potting soil (Biolan Oy, Kauttua, Finland). Seedlings were watered by absorption from the bottom every other day in a naturally illuminated greenhouse. Full-grown plants were transplanted into 4·5 L plastic pots filled with the same soil mix and maintained under natural light with midday photosynthetic photon fluxes

TABLE 1. *List of study species, including collection, habitat and distribution information*

Species	Collection site (collector)	Habitat and biogeography*
Trianthema portulacastrum L.	St. George, Utah, USA (R. Sage)	Moist or seasonally dry wetlands, sunny and dry areas along roadsides, in wastelands and in yards, neutral to alkaline soils, sandy and muddy coastal zones. Pantropical, widespread in Southeast Asia, tropical America and Africa. Altitude from sea level up to near 800 m.
Trianthema sheilae A.G. Mill. & Nyberg	Between Arga and Ahwar, Shabwa, Yemen (N. Kilian)	Sandy coasts, sandy slopes, amongst lava rocks or coral remains. Western coast of Saudi Arabia, the southern coast of Yemen, in southern Egypt, eastern Sudan and southern Eritrea. Altitude 10–2100 m.
Zaleya pentandra (L.) Jeffr.	Saudi Arabia (S. Liethe)	In open areas within woodlands, near riversides and in disturbed and cultivated areas. Throughout tropical Africa from northern South Africa to Egypt and Senegal; also in Palestine, Madagascar, Arabia, Iran and west Pakistan. Altitude 200–1600 m.

* Sources: *T. portulacastrum*: http://www.oswaldasia.org/species/t/trtpo/trtpo_en.html; *T. sheilae*: N. Kilian (personal communication); Hartmann *et al.* (2011); *Z. pentandra*: http://www.zimbabweflora.co.zw/speciesdata/species.php?species_id=123040, http://flora.huji.ac.il/browse.asp?lang=en&action=specie&specie=ZALPEN, http://www.efloras.org/florataxon.aspx?flora_id=5&taxon_id=250063404.

of approx. 900–1200 μmol m^{-2} s^{-1} (measured using a LI-250A light meter, LI-COR, Lincloln, NE, USA), 14/10 h light/dark photoperiod, approx. 30–35/20–25 °C day/night temperature regime and a relative humidity of 30–40 % (measured using a Thermo Hygrometer, Taylor Sybron, Mexico). Plants were watered every other day and fertilized biweekly with Ferti-Green (30 %:10 %:10 %, N:P:K) (Continental Research Corporation, St. Louis, MO, USA).

Leaf anatomy

Mature leaves (3–5 cm below the shoot tip) from approx. 2-month-old plants were used in all experiments. Leaf tissues sampled from the mid-portion of leaf blades (between the mid-rib and leaf margin) were fixed at room temperature in 1 % (v/v) glutaraldehyde in 100 mM (v/v) Na-cacodylate buffer (pH 7·2) solution (Muhaidat *et al.*, 2012). Samples were washed in buffer, post-fixed in 1 % (v/v) OsO_4 in Na-cacodylate buffer at 4 °C, dehydrated through a graded acetone series and infiltrated and embedded in Spurr's resin (Spurr, 1969).

For bright-field light microscopy, semi-thin sections (0·8 μm) were cut on a Reichert Ultracut ultramicrotome (Reichert-Jung, Vienna, Austria), dried onto poly-L-lysine-coated slides (100 μg mL^{-1}, mol. wt 560 000 Da) and stained with 1 % (w/v) toluidine blue O in 0·1 % (w/v) Na_2CO_3 (Muhaidat *et al.*, 2007). Sections were viewed under bright-field microscopy using Nikon ECLIPSE E400 (Nikon, Kawasaki, Japan) and photographed using a Nikon digital net camera DN100. For transmission electron microscopy (TEM), ultrathin sections (70–90 nm) were cut using the Ultracut ultramicrotome, and stained with 5 % (v/v) uranyl acetate and Reynolds lead citrate (Reynolds, 1963). Sections were examined under a Zeiss EM 10 CR electron microscope (Carl Zeiss NTS GmbH, Jena, Germany) and photographed using a plate and sheet film camera (3 1/4'' × 4'') (Carl Zeiss NTS GmbH, Jena, Germany). The TEM negatives were printed on ILFORD photographic papers (5'' × 7'') and scanned using an Epson GT 10 000 scanner (Model G650B, Seiko Epson Cord, Japan).

Light microscopic images were analysed for general patterning of leaf tissues, including arrangement of M and BS cells, and qualitative cell descriptions. Micrographs from TEM were taken in series for both M and BS cells. Numbers of chloroplasts and mitochondria per cell type profile were counted in 18 M cells and 18 BS cells from two leaves per species at ×5000 magnification. The level of granal development or thylakoid stacking in M and BS chloroplasts of each species was assessed by counting the number of stacked thylakoids in grana from 4–7 chloroplasts per cell type profile at ×16 000 magnification following Yoshimura *et al.* (2004). For cell wall thickness, measurements were made along BS–M interfacial walls off the primary pit fields, as wall thickness was greatly reduced in these areas (a common feature across all C_4 species). Recorded values are means of 40 measurements done manually on five TEM prints per species taken at ×20 000–25 000 total magnification for each species.

In situ *enzyme immunolocalization*

To clarify and establish PEP-CK involvement, the intercellular distribution patterns of five key C_4 enzymes (PEPC, PPdK, Rubisco, PEP-CK and NAD-ME) were examined in leaves of all three study species following Dengler *et al.* (1995) and Sudderth *et al.* (2007) for sample preparation and immunolocalization experiments. Polyclonal antisera used included anti-maize PEPC (courtesy of J. Berry, State University of New York, USA), anti-maize PPdK (courtesy of H. Sakakibara, Plant Science Center, Piken, Japan), anti-tobacco Rubisco holoenzyme (courtesy of N. G. Dengler, University of Toronto, Canada), anti-*Ananas comosus* PEP-CK (courtesy of F. Podestá, Universidad Nacional de Rosario, Rosario, Argentina) and anti-*Amaranthus hypochondriacus* α-subunit of NAD-ME (courtesy of N. G. Dengler, University of Toronto, Canada) IgG fractions. The specificity of each antiserum was ascertained by the supplier/contributing researcher, and tested in our study both by running control slides with diluting buffer lacking primary antiserum and by comparison localization experiments on transverse sections of *Amaranthus retroflexus* (C_4 NAD-ME) and *Melinis minutiflora* (C_4 PEP-CK) where enzymes accumulate in a known, tissue-specific manner (Edwards *et al.*, 2001).

Leaf tissues were fixed in a 3:1 (v/v) ethanol:acetic acid solution overnight at room temperature, dehydrated through graded ethanol–tertiary butyl alcohol mixtures and infiltrated and embedded in Paraplast (Wang *et al.*, 1992; Dengler *et al.*, 1995). Serial transverse sections (7 μm) were cut on a LEICA RM 2135 Rotary Microtome (Leica microsystems, Wetzler, Germany), mounted on poly-L-lysine-coated slides

and dried overnight. Following de-waxing, sections were rehydrated through an ethanol series and air-dried. They were rinsed and washed with Tris-buffered saline, pH 7·6 (Dako, Copenhagen, Denmark), covered with 3 % (v/v) H_2O_2 for 10 min, and subsequently washed with the same buffer. To prevent random, non-specific binding reactions, sections were pre-incubated for up to 15 min with a serum-free blocker (Dako). For each enzyme, sections were incubated for 1 h at room temperature in the primary antibody diluted in antibody diluting buffer, pH 7·6 (Dakocytomation Inc., Mississauga, ON, Canada) to 1:200 (v/v) Rubisco IgG, 1:2000 (v/v) PEPC IgG, 1:200 (v/v) PPdK IgG, 1:200 (v/v) NAD-ME IgG or 1:100 (v/v) PEP-CK IgG. Following incubation, all sections were washed and incubated for 30 min in a 1:10 (v/v) dilution of the EnVision + detection polymer secondary antibody (Dako). Binding reactions were visualized by incubating the sections with liquid 3,3-diaminobenzidine (DAB) and chromogen (Dako) for 8 min. Subsequently, the sections were rinsed with distilled H_2O and counterstained in 1 % (w/v) aqueous Azure B. Following a serial dehydration in ethanol, sections were mounted in Canada Balsam (Sigma-Aldrich Co. LLC, St. Louis, MO, USA), examined under bright-field microscopy, and digitally imaged.

Enzyme assays

Enzyme extraction and assay procedures were carried out as previously described by Muhaidat *et al.* (2007). Leaf tissue (0·1 g fresh weight) was frozen in liquid N_2 and immediately ground to a fine powder in acid-washed sand. A 1 mL aliuquot of extraction medium containing 50 mM HEPES-KOH (pH 7·5), 10 mM $MgCl_2$, 2·5 mM $MnCl_2$, 5 mM dithiothreitol (DTT), 0·2 mM Na_4-EDTA, 0·5 % bovine serum albumin (BSA) and 2·5 % (w/v) insoluble PVP (Ueno, 1992) was added, and grinding was continued on ice for about 30 s. Aliquots were taken for determination of chlorophyll content following the methodology of Wintermans and De Mots (1965). Residual homogenates were centrifuged at 14 000 rpm for approx. 30 s, and the supernatants were used for enzymatic assays. Activities of all enzymes were measured photometrically at 30 °C using a UV-VIS spectrophotometer at 340 nm (PG Instruments Limited, UK). The activity of each measured enzyme was calculated based on reaction rates recorded within a range where the increase in A_{340} nm was linear.

PEPC was assayed following NADH oxidation by coupling the carboxylase reaction with malate dehydrogenase (MDH) in a reaction medium containing 50 mM Bicine (pH 8·2), 2 mM DTT, 5 mM $MgCl_2$, 1 mM $NaHCO_3$, 1 mM Na_4-EDTA, 0·25 mM glucose-6-phosphate, 0·15 mM NADH, 2 U of MDH, 2 mM PEP, and enzyme extract (Muhaidat *et al.*, 2011). The reaction was initiated by addition of PEP. NADP-ME and NAD-ME were assayed following $NADP^+$ and NAD^+ reduction, respectively. The reaction medium for NADP-ME included 50 mM Tris–HCl (pH 8·2), 1 mM Na_4-EDTA, 20 mM $MgCl_2$, 0·5 mM $NADP^+$, 5 mM Na-malate, and enzyme extract. The reaction was initiated by addition of malate (Ku *et al.*, 1991). The assay medium for NAD-ME contained 25 mM HEPES-KOH (pH 7·2), 5 mM DTT, 0·2 mM Na_4-EDTA, 2·5 mM NAD^+, 5 mM Na-malate, 8 mM $(NH_4)_2SO_4$, 75 μM coenzyme A or 25 μM acetyl coenzyme A, 8 mM $MnCl_2$, 25 μM NADH, 1 U of MDH, and enzyme extract (Hatch and Kagawa, 1974; Hatch *et al.*, 1982). The reaction was started by addition of $MnCl_2$. PEP-CK was assayed in the carboxylase direction (Reiskind and Bowes, 1991; Chen *et al.*, 2002; Walker *et al.*, 2002) following NADH oxidation in a reaction mixture containing 100 mM HEPES-KOH (pH 7·0), 4 % (v/v) 2-mercaptoethanol, 100 mM KCl, 90 mM $NaHCO_3$, 5 mM PEP, 1 mM ADP, 10 μM $MnCl_2$, 4 mM $MgCl_2$, 0·14 mM NADH, 6 U of MDH, and enzyme extract. The reaction was initiated by addition of ADP.

Statistical analysis

Data were statistically analysed using SigmaStat software version 3·0 (Systat Inc., San Jose, CA, USA). Where appropriate and possible, raw variables were either square-root or log transformed to obtain data normality. Individual *t*-tests (or Wilcoxon tests for non-parametric data) were employed to evaluate differences between M and BS tissue variables within each species, and one-way analysis of variance (ANOVA) was used to compare multiple characteristics within a single tissue, or between all three species.

RESULTS

General leaf anatomy

Leaf blades of *T. portulacastrum* (Fig. 1A), *T. sheilae* (Fig. 1B) and *Z. pentandra* (Fig. 1C) are laminate and possess the atriplicoid form of *Kranz* anatomy. In all three species, individual vascular bundles are partially encircled by a prominent BS layer of large, cuboidal or wedge-shaped, compact cells (Fig. 1). The BS layer in all three species is incomplete on the abaxial side of the vein, and phloem cells are in contact with M cells. To the exterior of the BS layer is a concentrically arranged layer of palisade-like M cells exposed to intercellular airspace. The BS cells in all three species contain numerous, large, asymmetrically placed chloroplasts, which are centripetal in *T. portulacastrum* and *Z. pentandra*, and centrifugal in *T. sheilae*. In *T. sheilae*, a few chloroplasts are also dispersed along the radial and inner tangential walls of BS cells. In each of the three species, the palisade-like M cells contain fewer, smaller, peripherally located chloroplasts. *Trianthema portulacastrum* leaves show a single, discontinuous layer of large non-chlorenchymatous parenchyma cells adjacent to the adaxial epidermis, and two layers adjacent to the abaxial epidermis (Fig. 1A). These layers of large spongy parenchyma also have extensive intercellular airspace between individual cells. In leaves of *T. sheilae*, a single layer of widely spaced large non-chlorenchymatous parenchyma cells is present adjacent to both abaxial and adaxial surfaces (Fig. 1B). In comparison, leaves of *Z. pentandra* have a more typical bifacial anatomy, with M differentiated into three layers of palisade parenchyma (two adaxial and one abaxial), and two abaxial layers of spongy parenchyma exposed to intercellular airspace (Fig. 1C).

Ultrastructure of BS and M cells

Transmission electron microscopy of all species confirm observations of basic *Kranz* anatomy features by light

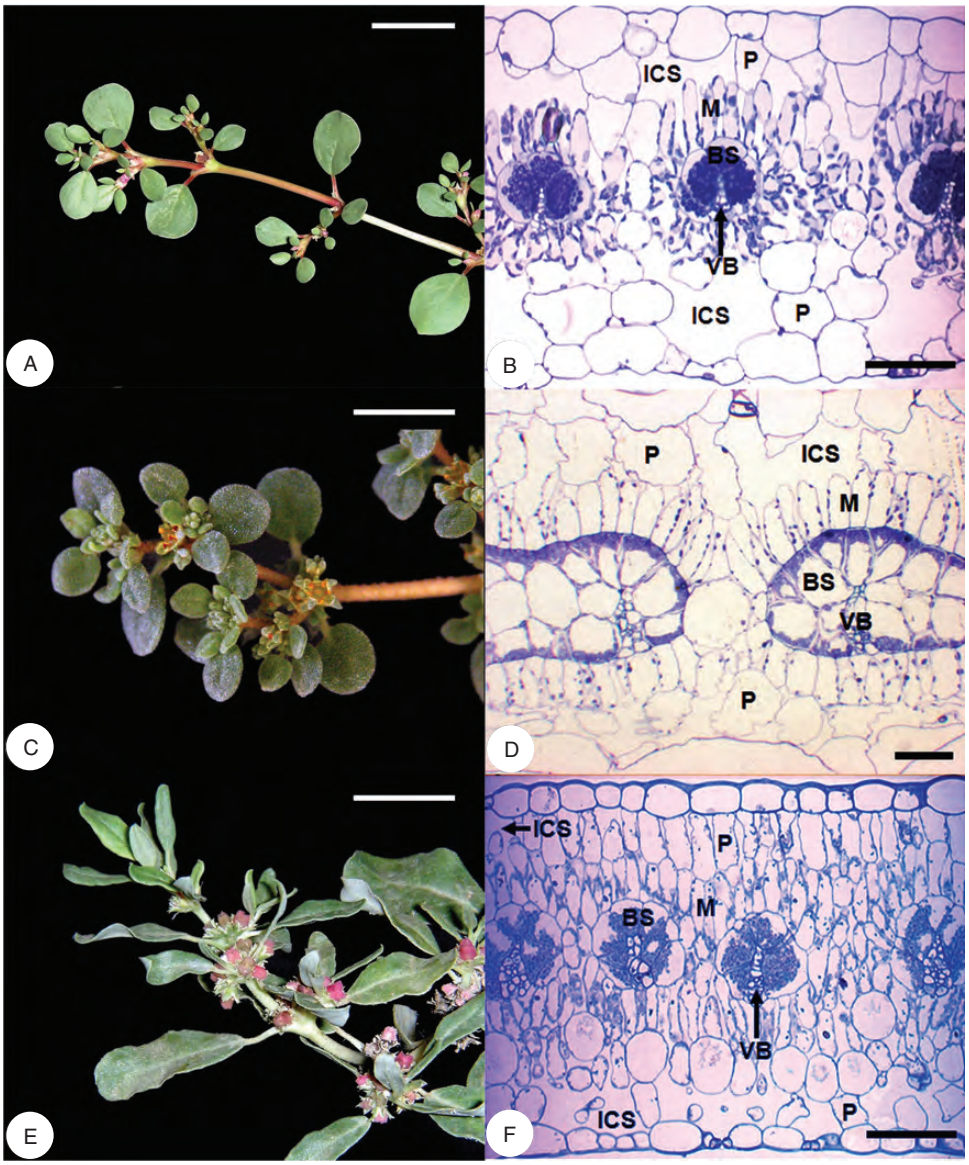

FIG. 1. Flowering shoots (left column) of *Trianthema portulacastrum*, *Trianthema sheilae* and *Zaleya pentandra* with corresponding light micrographs of leaf blade cross-sections (right column). (A, B) *Trianthema portulacastrum*. (C, D) *Trianthema sheilae*. (E, F) *Zaleya pentandra*. All species show atriplicoid-type *Kranz* anatomy where bundle sheath and mesophyll tissues form concentric layers around each vein. The bundle sheath layer is incomplete on the abaxial side of the vein, and shows asymmetric placement of chloroplasts. Abbreviations: BS, bundle sheath; ICS, intercellular space; M, mesophyll; P, non-chlorenchyamtous parenchyma; VB, vascular bundle. Scale bars: (A, C, E) = 2 cm; (B, D, F) = 100 μm.

microscopy and show further ultrastructural differences between BS and palisade-like M cells (Fig. 2). The size differences between BS and M organelles (chloroplasts, mitochondria and peroxisomes) are visually apparent and dimensions are consistently greater in BS cells than in M cells for all three species.

In *T. portulacastrum*, BS organelles are centripetally located while vacuoles are confined to the centrifugal sides of the BS cells, whereas organelles in the M cells are peripheral while vacuoles are centrally located (Fig. 2A). The BS chloroplasts are discoid or lenticular in shape, include starch and are largely agranal with only a few rudimentary grana of 2–3 stacked thylakoids (Fig. 2B, C). Comparatively, M chloroplasts are elongated, have little starch and contain conspicuous granal development consisting mostly of 4–7 stacked thylakoids (Fig. 2D). Grana of lower and higher thylakoid stacking levels in M chloroplasts are less common. In the BS, mitochondria are numerous, distributed between BS chloroplasts (Fig. 2B, E), and are spherical to slightly oval in shape with tubular cristae (Fig. 2E, inset). Physical contact between BS chloroplasts and mitochondria is not apparent. The mitochondria in M cells are smaller, less numerous and peripherally located (not shown).

In leaves of *T. sheilae*, BS organelles are largely centrifugally located, while vacuoles occupy the centripetal portions of the BS cells (Fig. 2F). In M cells, organelles are peripheral with a

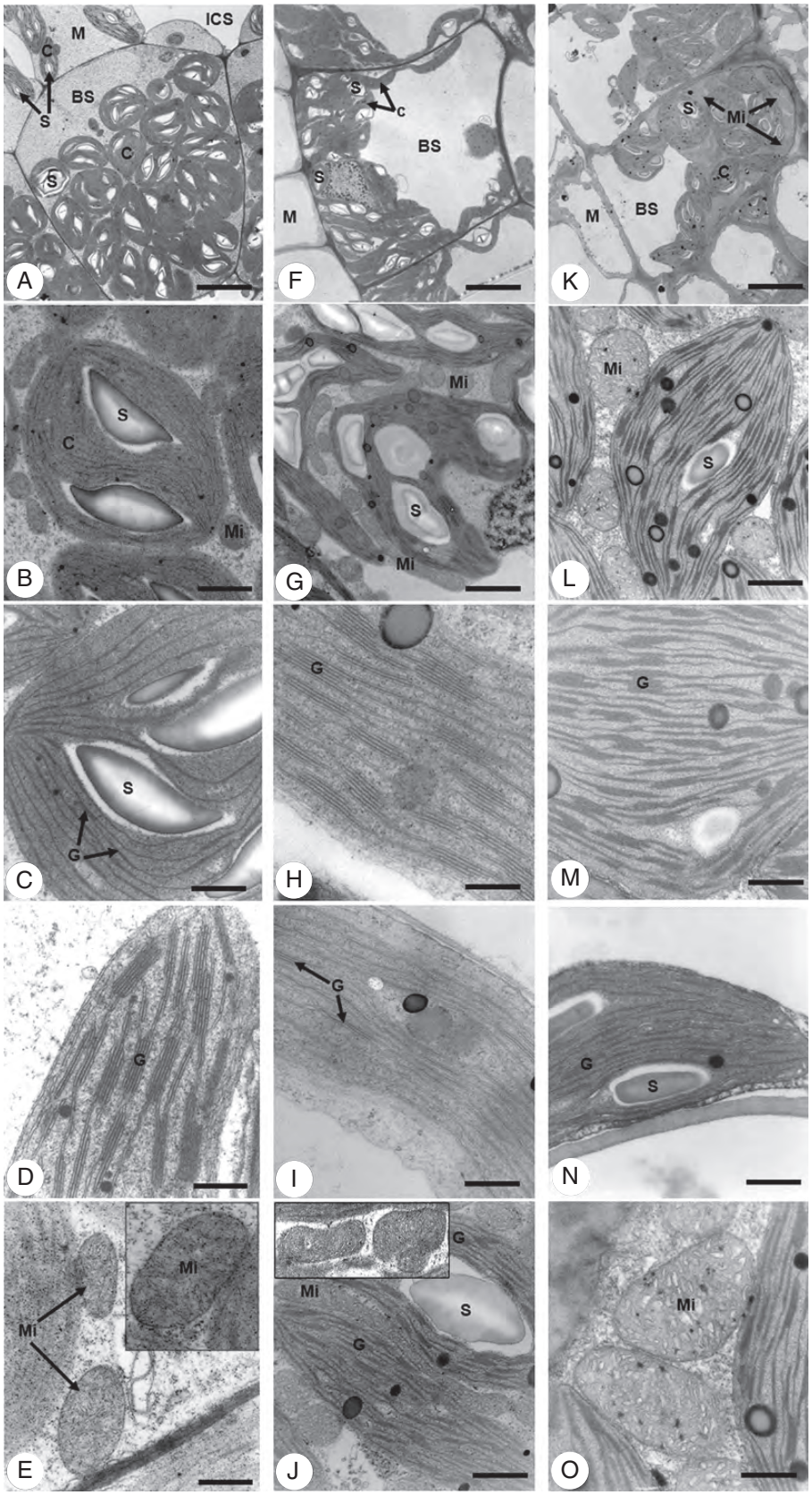

FIG. 2. Transmission electron micrographs of leaf blade cross-sections of *Trianthema portulacastrum* (left column), *Trianthema sheilae* (middle column) and *Zaleya pentandra* (right column) illustrating ultrastructural features of bundle sheath and mesophyll cells. (A, F, K) Bundle sheath cells and portions of adjoining

TABLE 2. *Mean counts of organelles and numbers of stacked thylakoids per granum in chloroplasts of bundle sheath (BS) and mesophyll (M) cells in C_4* Trianthema portulacastrum*,* Trianthema sheilae *and* Zaleya pentandra *(± s.e.)*

Species/tissue type	Chloroplasts (*n*)*	Mitochondria (*n*)*	Peroxisomes (*n*)*	Thylakoids/granal stack (*n*)†
BS tissue				
Trianthema portulacastrum	22·6 ± 0·5[a]	16·3 ± 0·2[a]	2·8 ± 0·2[a]	2·3 ± 0·03[a]
Trianthema sheilae	20·7 ± 0·5[b]	39·3 ± 1·0[b]	2·1 ± 0·2[b]	5·0 ± 0·1[b]
Zaleya pentandra	16·1 ± 0·4[c]	32·8 ± 1·4[c]	3·1 ± 0·2[a]	4·1 ± 0·1[c]
M tissue				
Trianthema portulacastrum	6·4 ± 0·4[a]	5·4 ± 0·3[a]	0·4 ± 0·1[NS]	4·6 ± 0·1[a]
Trianthema sheilae	5·6 ± 0·3[a]	8·7 ± 0·4[b]	0·3 ± 0·1[NS]	2·7 ± 0·1[b]
Zaleya pentandra	8·9 ± 0·3[b]	6·3 ± 0·4[a]	0·3 ± 0·1[NS]	2·6 ± 0·1[b]

Different letters indicate significant BS or M organelle differences between species using one-way ANOVA ($P < 0·001$). NS, non-significant.
* $n = 18$ cells per tissue type per species.
† $n = 4–7$ chloroplasts per tissue type per species.

centrally located vacuole (not shown). The BS chloroplasts are elongated, include starch and have prominent, well-developed grana with as many as 11 stacked thylakoids per granum (Fig. 2G, H). Grana with lower levels of thylakoid stacking are also present; however, rudimentary grana of 2–3 stacked thylakoids are least abundant. The M chloroplasts are also elongated, but have little starch, and are grana deficient (Fig. 2I). They are predominated by individual thylakoids or grana of paired thylakoids, and grana of higher stacking levels are rare (Fig. 2I). Mitochondria in BS cells are numerous, large in size and spherical to elongated in shape, with many tubular translucent cristae (Fig. 2G, J). These are distributed mainly between the interior chloroplasts and along the radial and inner tangential BS walls, while the outermost portions of BS cells lack mitochondria. Close contact between mitochondria and chloroplasts in BS cells of *T. sheilae* is consistently observed (Fig. 2J, inset). In M cells, mitochondria are smaller, fewer and evenly distributed around the peripheral walls (not shown).

Leaves of *Z. pentandra* exhibit BS organelles that are centripetally located, while vacuoles are found toward the centrifugal portion of the BS cell (Fig. 2K). In M cells, organelles are peripherally located while the vacuole is central (not shown). The chloroplasts of BS cells vary from lenticular to partially elongate (Fig. 2K), and contain starch and well-developed grana of mostly 4–6 stacked thylakoids (Fig. 2L, M). Grana of lower and higher (up to 12) levels of thylakoid stacking are less common. In contrast, M chloroplasts are elongated and exhibit reduced levels of granal development, consisting predominantly of 2–3 stacked thylakoids (Fig. 2N). The mitochondria in BS cells are numerous and largely spherical to oval in shape, with mostly vesicular cristae, and are distributed between BS chloroplasts (Fig. 2L, O). There is also apparent physical contact between BS chloroplasts and mitochondria. In M cells, mitochondria are fewer, smaller in size and distributed along the peripheral walls (not shown).

Quantitative evaluation of organelles, thylakoid stacking and cell wall thickness

In all three species, BS cells contain significantly more chloroplasts, mitochondria and peroxisomes per cell profile than M cells ($P < 0·001$; Table 2, *t*-tests not indicated). For each species, the number of organelles within each tissue is also significantly different ($P < 0·001$; Table 2, one-way ANOVA tests not indicated). In *T. portulacastrum*, the number of BS chloroplasts per cell profile is 1·4-fold greater than the number of mitochondria, whereas in *T. sheilae* and *Z. pentandra*, the number of BS mitochondria per cell profile is 2-fold greater than the number of chloroplasts. In M tissues of all three species, the numbers of chloroplasts and mitochondria per M cell profile are relatively more comparable. Numbers of peroxisomes per cell profile in both BS and M tissues are substantially lower than the numbers of either chloroplasts or mitochondria in each species. Comparing the three species shows that organelle numbers differ, particularly in BS tissue ($P < 0·001$; Table 2). The numbers of BS chloroplasts per cell profile are highest in *T. portulacastrum* relative to *T. sheilae* and *Z. pentandra*. In contrast, numbers of BS mitochondria per cell profile are higher in *T. sheilae* and *Z. pentandra* than in *T. portulacastrum*. Numbers of peroxisomes per BS cell profile are higher in both *T. portulacastrum* and *Z. pentandra*, compared with *T. sheilae*. Numbers of M organelles show fewer differences among the three species.

Granal development between BS and M chloroplasts, as assessed by thylakoid stacking, is significantly different within each species ($P < 0·001$; Table 2, *t*-tests not indicated). In *T. portulacastrum*, the number of stacked thylakoids per grana in BS chloroplasts is 2-fold lower than in M chloroplasts. In comparison, in both *Z. pentandra* and *T. sheilae*, the number of thylakoids per granal stack in BS chloroplasts is 1·5- to 2-fold higher, respectively, than in M chloroplasts. Comparing chloroplasts among all three species shows that the

mesophyll cells showing centripetal placement of organelles in bundle sheath of *T. portulacastrum* (A) and *Z. pentandra* (K), compared with centrifugal placement in *T. sheilae* (F). (B, G, L) Higher magnifications of bundle sheath cells showing the distribution of chloroplasts, starch grains and mitochondria. Physical contact between chloroplasts and mitochondria in bundle sheath cells is observed in *T. sheilae* (G) and *Z. pentandra* (L). (C, H, M) Higher magnifications of bundle sheath chloroplasts showing granal stacking. (D, I, N) Higher magnifications of mesophyll chloroplasts showing starch grains and granal stacking. (E, J, O) Higher magnification of bundle sheath mitochondria showing cristae, which are numerous, pronounced and translucent in *T. sheilae* (J) and *Z. pentandra* (O). (E, J insets) show additional higher magnification images of mitochondria. Abbreviations: BS, bundle sheath; C, chloroplast; G, granal stack; ICS, intercellular space; M, mesophyll; Mi, mitochondria; S; starch grain. Scale bars: (A) = 4 μm; (B) = 0·63 μm; (C, E) = 0·32 μm; (D) = 0·2 μm; (E inset), (M, N, O) = 0·16 μm; (F) = 5 μm; (G) = 2 μm; (H) = 0·1 μm; (I, J and inset) = 0·5 μm; (K) = 4 μm; (L) = 0·25 μm.

level of thylakoid stacking is significantly different, particularly in granal development of BS chloroplasts ($P < 0{\cdot}001$; Table 2). Thylakoid stacking in BS chloroplasts is 1·8- to 2·2-fold greater in both *Z. pentandra* and *T. sheilae*, respectively, than in *T. portulacastrum*. In contrast, the level of thylakoid stacking in M chloroplasts of *T. portulacastrum* is 1·7-fold higher than in both *T. sheilae* and *Z. pentandra.*

Cell walls of BS are visually thicker than M cell walls in all three species (Fig. 3, arrows) and BS wall thickening is greatest at sites exposed to intercellular space (not shown). The BS cell walls of *T. sheilae* (Fig. 3B) are pronouncedly thicker than those of both *T. portulacastrum* (Fig. 3A) and *Z. pentandra* (Fig. 3C). In comparison, M cell walls of all three species appear of relatively similar thickness. The average total thickness of walls at the BS–M interface is significantly different among all three species ($P < 0{\cdot}001$; Supplementary Data Fig. S1). Average BS–M wall thickness is 1·8- to 3·7-fold greater in *T. sheilae* at 0·53 μm compared with 0·30 μm in *Z. pentandra* and 0·14 μm in *T. portulacastrum*. In each species, aggregates of plasmodesmata in primary pit fields traverse the BS–M interfacial wall region (Supplementary Data Fig. S2).

Activities of key C_4 photosynthetic enzymes

In vitro activities of four key enzymes involved in the C_4 pathway (PEPC, NADP-ME, NAD-ME and PEP-CK) differ between all three study species, particularly in C_4 acid decarboxylating enzyme activities (Table 3). High levels of PEPC activity are found in leaves of *Trianthema* and *Zaleya* species, typical and similar to the comparison C_4 species. Leaves of *T. portulacastrum* have high activities of both NADP-ME and PEP-CK, and comparatively low activity of NAD-ME. NADP-ME activity in *T. portulacastrum* is 1·5-fold higher than that of PEP-CK, and 22-fold higher than that of NAD-ME. Leaves of *T. sheilae* demonstrate high NAD-ME activity, and low activities of NADP-ME and PEP-CK. NAD-ME activity in *T. sheilae* is 8- to 16-fold higher than that of PEP-CK and NADP-ME, respectively. Leaves of *Z. pentandra* have high NAD-ME and PEP-CK activities, and low NADP-ME activity. NAD-ME activity in *Z. petandra* is 1·2-fold higher than that of PEP-CK, and 8-fold higher than that of NADP-ME. Relative to each other, PEP-CK activity is substantially higher in both *Z. pentandra* and *T. portulacastrum* (6- to 10-fold, respectively), than in *T. sheilae*.

In situ *immunolocalizations of photosynthetic enzymes*

Immunolocalizations of Rubisco, PEPC, PPdK, PEP-CK and NAD-ME in leaves of *T. portulacastrum*, *T. sheilae* and *Z. pentandra* show cell-specific accumulation patterns as indicated by a brown colour precipitate (Fig. 4). This is similar to comparison C_4 species (NAD-ME *Amaranthus retroflexus*, not shown; PEP-CK *Melinis minutiflora*, see Supplementary Data Fig. S3), while control leaf sections showed negligible, non-specific labelling (not shown). The BS cells in all three species are densely and specifically labelled by the antibody to Rubisco, with labelling in BS chloroplasts (Fig. 4A, F, K). Labelling for Rubisco in M and spongy parenchyma cells is absent. Specific labelling for PEPC is observed in the M layer enclosing the BS tissue of all three species, but no labelling is detected in either BS cells or distant M/spongy parenchyma cells (Fig. 4B, G, L). The pattern of labelling for PPdK is similar to that for PEPC in all three species, and chloroplasts in M cells adjacent to the BS are selectively labelled by PPdK antiserum, while no labelling is found in other cell types (Fig. 4C, H, M). Specific labelling for the decarboxylating enzymes PEP-CK and NAD-ME is observed in BS cells of all three species to different extents. Labelling for PEP-CK is strong in the BS cells of *T. portulacastrum* and *Z. pentandra* (Fig. 4J, L), while it is much weaker and predominantly limited to the interior of BS chloroplasts in *T. sheilae*

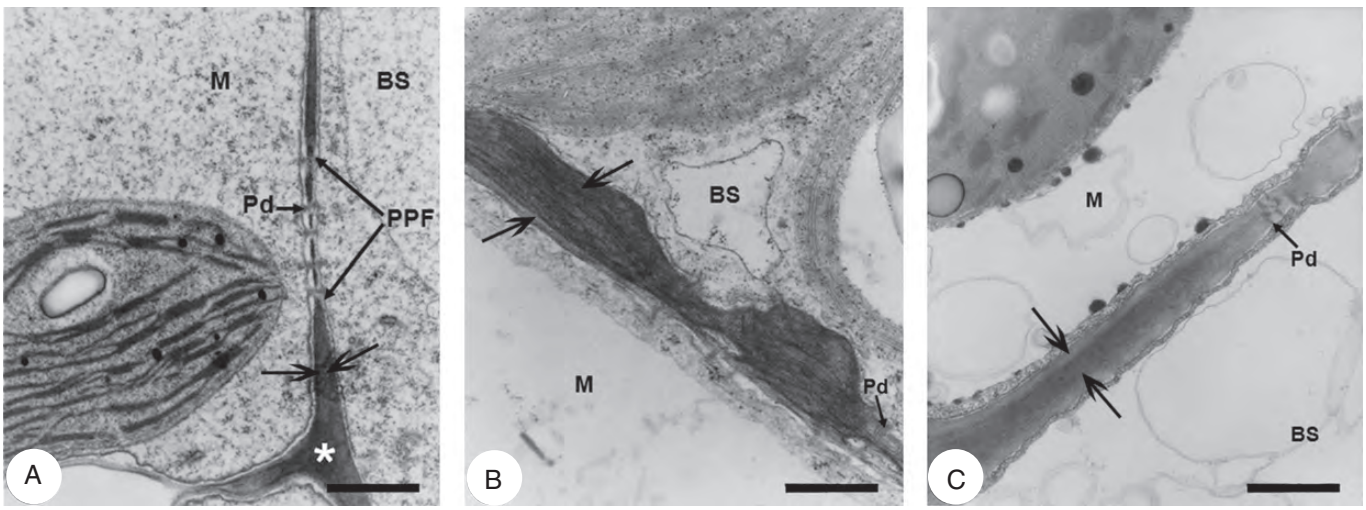

FIG. 3. Transmission electron micrographs of leaf blade cross-sections showing the bundle sheath–mesophyll wall interface in *Trianthema portulacastrum*, *Trianthema sheilae* and *Zaleya pentandra*. (A) *Trianthema portulacastrum* wall interface with pitting and plasmodesmata. (B) *Trianthema sheilae* wall interface with pitting and plasmodesmata showing pronounced wall thickening in the common wall between mesophyll and bundle sheath. (C) *Zaleya pentandra* wall interface with pitting and plasmodesmata. Abbreviations: BS, bundle sheath; M, mesophyll; Pd, plasmodesmata; PPF, primary pit field. Scale bars: (A) = 0·5 μm; (B) = 0·25 μm; (C) = 0·4 μm.

TABLE 3. *Mean activities of C_4 photosynthetic enzymes in crude leaf extracts (± s.e.) of study C_4 species* Trianthema portulacastrum, Trianthema sheilae, Zaleya pentandra, *and comparison C_3 and C_4 species* (n = *3–5*)

Species	Photosynthetic type, sub-type	Enzyme activity (μmol mg chlorophyll^{-1} h^{-1})			
		PEPC	NADP-ME	NAD-ME	PEP-CK
Study species					
Trianthema portulacastrum	C_4, NADP-ME*	1340·2 ± 8·4	767·2 ± 4·7	35·1 ± 1·4	518·5 ± 4·2
Trianthema sheilae	C_4, NAD-ME†	1252·5 ± 7·4	26·6 ± 1·9	408·4 ± 12·8	53·5 ± 2·0
Zaleya pentandra	C_4, NAD-ME*	1192·7 ± 10·3	45·8 ± 3·7	383·2 ± 8·1	319·4 ± 4·4
Comparison species					
Euphorbia peplus L.	C_3	37·5 ± 3·1	19·9 ± 2·3	11·1 ± 0·9	8·4 ± 0·5
Zea mays L.	C_4, NADP-ME	1246·0 ± 14·1	719·1 ± 3·3	111·6 ± 4·1	152·2 ± 4·1
Amaranthus retroflexus L.	C_4, NAD-ME	1095·1 ± 15·6	84·1 ± 4·6	679·8 ± 10·7	31·0 ± 0·2
Cleome gynandra L.	C_4, NAD-ME	1130·7 ± 20·5	8·3 ± 0·3	648·2 ± 5·4	246·6 ± 4·4
Melinis minutiflora Beauv.	C_4, PEP-CK	1030·5 ± 8·6	12·8 ± 0·6	119·3 ± 4·1	572·3 ± 6·0

* Designation based on Muhaidat *et al.* (2007)
† Designation based on this study.
PEPC, phospho*enol*pyruvate carboxylase; NADP-ME, NADP-malic enzyme; NAD-ME, NAD-malic enzyme; PEP-CK. phospho*enol*pyruvate carboxykinase.

(Fig. 4I; Supplementary Data Fig. S3). In comparison, labelling for NAD-ME is much stronger in BS cells of *T. sheilae* and *Z. pentandra* (Fig. 4J, O) compared with *T. portulacastrum* (Fig. 4E). In addition, labelling for NAD-ME appears strongest within the innermost BS chloroplasts of *T. sheilae* (Fig. 4J), while this is not observed in either *T. portulacastrum* or *Z. pentandra*.

DISCUSSION

This study confirmed two biochemical sub-types of C_4 photosynthesis (NADP-ME and NAD-ME) within the Sesuvioideae (Aizoaceae) and significant involvement of PEP-CK in both sub-types based on surveys of leaf anatomy, and activity and immunolocalizations of key C_4 enzymes. Both *T. portulacastrum* and *Z. pentandra* are classified as NADP-ME and NAD-ME sub-types, respectively, based on the high levels of each enzyme (Muhaidat *et al.*, 2007), and, with the current evidence, *T. sheilae* should be classified as NAD-ME sub-type. The clear presence of PEP-CK through enzyme immunolocalizations and activity assays was observed in both NADP-ME *T. portulacastrum* and NAD-ME *Z. petandra*, indicating putative recruitment of this enzyme (or pathway) in C_4 photosynthesis of eudicot species, regardless of the predominating decarboxylation enzyme.

Leaf anatomy related to recruitment of PEP-CK

The presence of atriplicoid-type *Kranz* anatomy in all three C_4 species underscores common requirements for C_4 functioning, independent of differentiation in C_4 biochemical sub-type. Alongside tissue arrangement, anatomical specializations, such as interior placement of mitochondria with respect to chloroplasts and very minimal exposure of BS to intercellular spaces, were found in all three species. Atriplicoid-type *Kranz* anatomy is one of the most widespread and prevalent forms of anatomical specialization in the C_4 eudicots, suggesting extensive evolutionary convergence (Muhaidat *et al.*, 2007). While this convergence refers to the overall arrangement of tissues (i.e. concentric rings of tissues around veins), it does not necessarily reflect smaller scale anatomical differences, such as chloroplast and mitochondrial arrangement, numbers or sizes, thylakoid stacking or cell wall interface thickness. These finer anatomical distinctions instead are generally associated with the biochemical sub-type of C_4 photosynthesis, and previous studies of C_4 grasses and sedges have shown that anatomy has good predictive value for sub-type biochemistry and ecology (Dengler and Nelson, 1999).

The centrifugal clustering of chloroplasts in the BS cells occurred only in NAD-ME *T. sheilae*. In C_4 grasses, this trait is often associated with NADP-ME and PEP-CK sub-types (Dengler and Nelson, 1999). In contrast, BS chloroplast placement in C_4 eudicots tends to be independent of biochemical sub-type (see Muhaidat *et al.*, 2007), and was also observed in this study. Centrifugal positioning of organelles in BS cells of C_4 eudicots is unusually rare, and occurs irrespective of biochemical sub-type. For instance, other C_4 eudicots with centrifugally located chloroplasts in BS cells include NADP-ME *Halothamnus glaucus*, NAD-ME *Suaeda eltonica*, *S. acuminate* and *S. cochlearifolia*, and C_4 subspecies of NAD-ME *Tecticornia indica* (Chenopodiaceae) (Voznesenskaya *et al.*, 2007, 2008). Within the Sesuvioideae, C_4 *Trianthema triquetra* also possesses centrifugally located BS organelles, although the C_4 biochemical sub-type of this species is currently unknown (Carolin *et al.*, 1978). The evolutionary or ecological significance of this atypical attribute in C_4 eudicots is unknown (Dengler and Nelson, 1999; Voznesenskaya *et al.*, 2006, 2007, 2008), but does not appear to relate to recruitment of PEP-CK.

In this study, many observed ultrastructural differences followed 'classical' characteristics of NADP-ME and NAD-ME sub-types, with the exception of BS chloroplast location (Gutierrez *et al.*, 1974; Hatch *et al.*, 1975; Hatch, 1987; Dengler and Nelson, 1999; Voznesenskaya *et al.*, 1999; Yoshimura *et al.*, 2004; Edwards and Voznesenskaya, 2011). Mitochondria numbers relative to chloroplasts in BS cells followed biochemical sub-type, and both NAD-ME species (*T. sheilae* and *Z. petandra*) had the highest numbers of large BS mitochondria (Table 2). The BS chloroplasts and

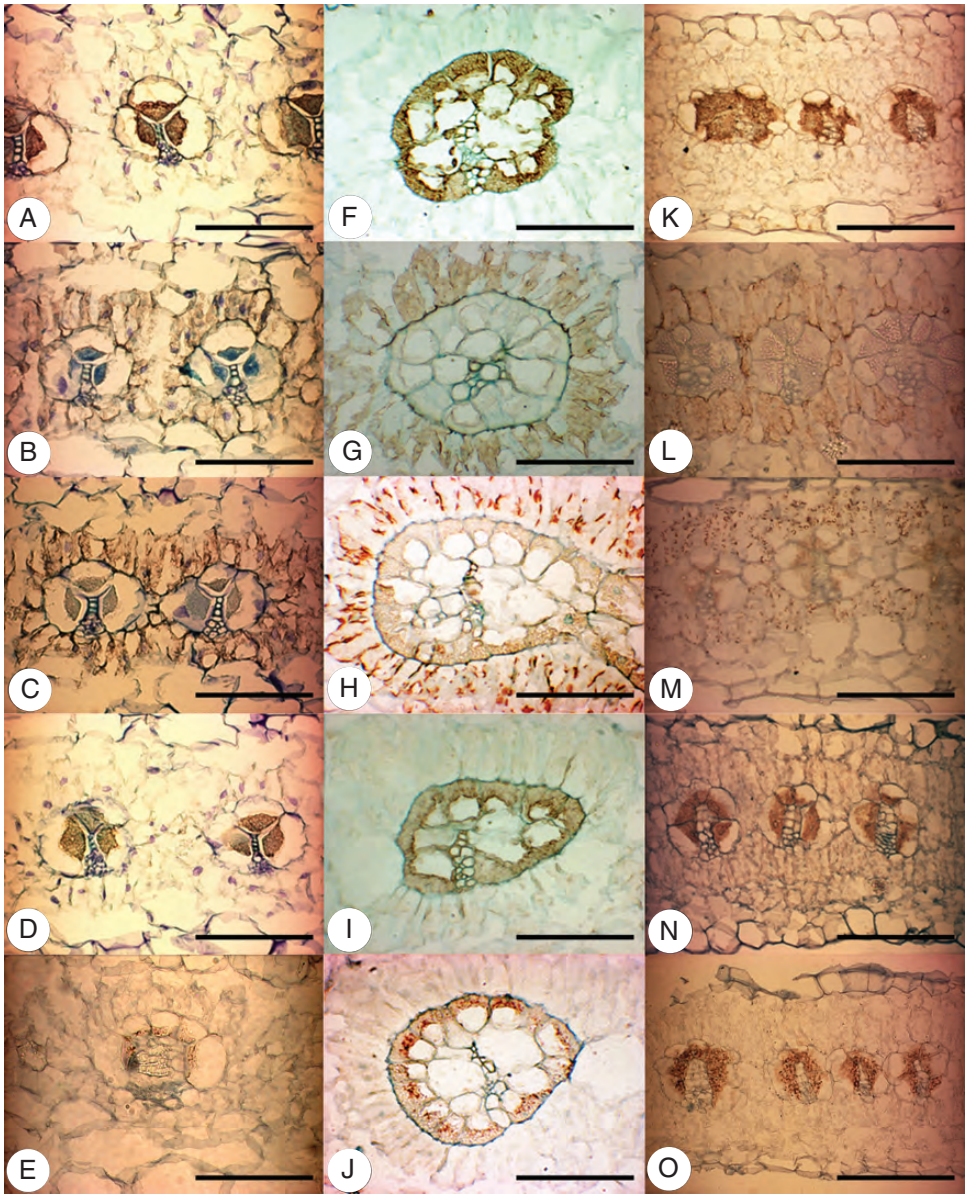

FIG. 4. Light micrographs of *in situ* immunolocalizations of photosynthetic enzymes in cross-sections through leaves of *Trianthema portulacastrum* (left column), *Trianthema sheilae* (middle column) and *Zaleya pentandra* (right column). Tissue-specific immunolabelling is indicated by the brown precipitate. (A, F, K) Rubisco in bundle sheath cells. (B, G, L) PEPC in mesophyll cells encircling bundle sheath cells. (C, H, M) PPDK in mesophyll cells encircling bundle sheath cells. (D, I, N) PEP-CK in bundle sheath cells. (E, J, O) NAD-ME in bundle sheath cells. Scale bars = 100 μm.

mitochondria of the NAD-ME species also had close contact, whereas this was not observed in the NADP-ME *T. portulacastrum* (Fig. 2). Chloroplast thylakoid stacking in different tissues coincided with the principal biochemical sub-type, as both NAD-ME species had higher thylakoid stacking in BS chloroplasts and lower thylakoid stacking in M chloroplasts (Table 2). The increased granal development in BS chloroplasts and greater numbers of mitochondria observed in the NAD-ME species compared with the NADP-ME species in this study are characteristics which correlate with variations in the energy forms required to sustain a given type of C_4 metabolism in BS cells (Edwards and Walker, 1983; Kanai and Edwards, 1999; Takabayashi *et al.*, 2005).

Only a few ultrastructural features appeared to be involved with the presence of the PEP-CK pathway. Higher numbers of M chloroplasts and BS peroxisomes occurred alongside increased PEP-CK activity, where these organelle numbers were greater in *T. portulacastrum* and *Z. petandra* than in *T. sheilae* (Table 2). This increase in M chloroplasts could be associated with maximizing PPdK activity to meet a greater C_3 influx back into M cells. A higher influx would be created by multiple C_4 acid decarboxylation modes in the BS cells, including NADP-ME or NAD-ME along with PEP-CK, and is a possibility that requires further investigation. In particular, thylakoid stacking in BS chloroplasts and the level of PEP-CK activity followed opposing patterns where

PEP-CK activity: *T. portulacastrum* > *Z. pentandra* > *T. sheilae*, was opposite to the degree of granal stacking in BS chloroplasts: *T. portulacastrum* < *Z. pentandra* < *T. sheilae* (Table 2). This is in contrast to the high degree of thylakoid stacking in BS chloroplasts of C_4 PEP-CK grasses which is needed for increased photosystem II (PSII) and non-cyclic electron flow activities producing both ATP and NADPH (Edwards and Walker, 1983; Edwards and Voznesenskaya, 2011). The coincidence of enhanced PEP-CK activity in both NADP-ME and NAD-ME C_4 eudicots is also inconsistent with the previously outlined progressive pattern of PEP-CK engagement in correlation with the degree of thylakoid stacking in BS chloroplasts (Wingler *et al.*, 1999; Voznesenskaya *et al.*, 2006), and independent of PSII content of the BS chloroplasts (see Furbank, 2011).

Cell wall thickness, particularly at the M–BS interface, did not appear to be associated with recruitment of PEP-CK. Cell walls were thickest in NAD-ME *T. sheilae*, while cell walls of NAD-ME *Z. pentandra* had intermediate values compared with NADP-ME *T. portulacastrum*. Cell wall thickness may instead relate partially to the centrifugal positioning of BS organelles, as observed in *T. sheilae*. This pattern was also apparent in the total activity of the three decarboxylating enzymes: *T. sheilae* < *Z. pentandra* < *T. portulacastrum*. Thus, cell wall thickness may be a trade-off for the three species where the lower total sum of C_4 acid decarboxylating enzyme activities may require a thicker wall to maintain, or retain, as high CO_2 levels in BS cells as possible and reduce potential CO_2 leakage. In *T. sheilae*, the distribution of the BS mitochondria (the site of NAD-ME activity) was also restricted to the region of interior chloroplasts and along the radial and inner BS walls. Consequently, CO_2 released from mitochondria can be recaptured by the overlying BS chloroplasts, thus greatly reducing diffusive loss of CO_2.

Contribution of PEP-CK to other C_4 pathways

In both NADP-ME *T. portulacastrum* and NAD-ME *Z. petandra*, PEP-CK levels were high, comparable with those reported for C_4 PEP-CK grasses (Gutierrez *et al.*, 1974; Hatch *et al.*, 1975; Prendergast *et al.*, 1987). For both species, immunolocalization of PEP-CK was particularly strong in BS cells, and consistent with enzyme activity records (Fig. 4, Table 3). The PEP-CK levels ranged from 47 to 85 % of the predominating decarboxylating enzyme (NADP-ME or NAD-ME), providing robust evidence for the co-occurrence of a PEP-CK C_4 shuttle in C_4 eudicots. Additional C_4 eudicot species demonstrating high PEP-CK activity using enzyme assays include NADP-ME *Boerhavia coccinea* and *B. domnii* (Nyctaginaceae) and NAD-ME *Cleome gynandra* (Table 3; Marshall *et al.*, 2007; Muhaidat *et al.*, 2007; Sommer *et al.*, 2012). Significant activity and expression level of PEP-CK has also been reported in NAD-ME *Portulaca oleracea* (Portulacaceae) (Lara *et al.*, 2004) based on enzyme assays and western blot analysis of the decarboxylating enzymes, although this was not confirmed in a study by Voznesenskaya *et al.* (2010). In each of these C_4 eudicot species, BS organelles were observed to be centripetally located. As similar results are beginning to be uncovered in other C_4 eudicot lineages (see Sommer *et al.*, 2012), we conclude that our values and observations are accurate and draw attention to the unusually high levels of PEP-CK in C_4 eudicot species, suggesting that multiple pathways of decarboxylation coexist.

Finding significant PEP-CK activity in a range of C_4 eudicot species could be attributed to the assay method used for the enzyme. The conventional technique for PEP-CK detection in C_4 plants uses radioisotopes with the assay proceeding in the decarboxylase direction. Radiometric procedures for enzymic studies are lengthy and can give false results through curtailed enzyme activity (Sharkey *et al.*, 1991). In a previous study, Muhaidat *et al.* (2007) followed newer, reliable methods (Reiskind and Bowes, 1991; Walker *et al.*, 1997, 2002; Chen *et al.*, 2002) which are spectrophotometric rather than radiometric. In this study, following the same spectrophotometric methods, the PEP-CK activity values for the C_3 and C_4 comparison species were similar to those of previous reports (Gutierrez *et al.*, 1974; Prendergast *et al.*, 1987). Independent assays of PEP-CK activity in *Cleome gynandra* (Table 3) yielded values similar to previously published records (Marshall *et al.*, 2007; Muhaidat *et al.*, 2007). In support of these enzyme activity assays, immunolocalization studies of PEP-CK protein in *Melinis minutiflora* and *C. gynandra* indicated that the protein is specifically abundant in the BS layer (Supplementary Data Fig. S3). Given that PEP-CK catalyses a reversible reaction, Chen *et al.* (2002) reported that the enzyme could operate as a carboxylase *in vivo* if assayed at the physiological concentrations of the metal ions Mn^{2+} and Mg^{2+}. Thus, evaluating the reliability of the radiochemical and the photometric methods for PEP-CK assays in C_4 eudicots, and quantifying protein levels through western blots to reassess formerly established biochemical designations is therefore necessary and may shed further light on PEP-CK involvement in other C_4 eudicots.

Operation of a PEP-CK sub-type C_4 shuttle in both NAD-ME and NADP-ME C_4 eudicots raises questions regarding potential energy sources required for the cytosolic PEP-CK reaction. The PEP-CK reaction is known to be ATP dependent (Edwards and Walker, 1983). This energy requirement is proposed to be largely met by oxidizing malate via the engagement of an NAD-ME type C_4 shuttle producing ATP in the mitochondria in addition to CO_2 (Burnell and Hatch, 1988; Carnal *et al.*, 1993; Heldt and Piechulla, 2011). Biochemical surveys in C_4 grasses revealed that NAD-ME functioning at a level of 25–40 % of that of PEP-CK meets the energy demands of the PEP-CK reaction in PEP-CK sub-type grasses (Kanai and Edwards, 1999). In addition to this, Furbank (2011) noted that little evidence exists for 'pure' PEP-CK, i.e. without operation of an NAD-ME cycle to provide ATP. Using this as a baseline, the activity level of NAD-ME in *Z. pentandra* in this study should be more than sufficient to support the PEP-CK reaction (Table 3; Voznesenskaya *et al.*, 2006); however, this situation is unlikely in NADP-ME *T. portulacastrum*. Proposed alternative pathways of meeting the ATP demand of PEP-CK in NADP-ME species suggested by Kanai and Edwards (1999) include cellular respiration or the oxidation of triose phosphate to 3-phosphoglycerate. Increased demand on cyclic

photophosphorylation by development of largely agranal BS chloroplasts may also play a role, as observed in *T. portulacastrum* in this study.

Evolution of C_4 photosynthesis in Sesuvioideae

There has been increasing interest in exploring origins and modes of C_4 diversification in angiosperms, and reconstructing specific evolutionary paths to C_4 photosynthesis (Sage, 2004; McKown and Dengler, 2007; Gowik and Westhoff, 2011; Khoshravesh *et al.*, 2012). C_4 eudicots offer unusual opportunities for insight into convergent evolution, and to test generalizations largely made on C_4 monocots. Among C_4 eudicots, Sesuvioideae (Aizoaceae) may be a new model for inferring patterns and trends of C_4 photosynthesis evolution, particularly as C_4 photosynthesis has arisen fairly frequently in this group (Sage, 2004). Anatomical and biochemical data thus far demonstrate that closely related C_4 species occurring in similar environments share *Kranz* anatomy type but belong to different biochemical sub-types and differ in ultrastructural features (see also Carolin *et al.*, 1978). In addition, two species showed significant activity of PEP-CK, and may be useful for understanding the ecological or selective forces, such as increasing seasonality or drier climates, in PEP-CK appearance or expression in Sesuvioideae. This strong presence of PEP-CK in both *Trianthema* and *Zaleya* suggests the possibility that other species with significant PEP-CK recruitment may exist elsewhere within the Sesuvioideae. Analysing a larger collection of C_4 eudicot species, including additional Sesuvioideae species, will enhance our understanding of modes of C_4 evolution in eudicots and biochemical diversification including PEP-CK in combination or as an alternative decarboxylase for C_4 photosynthesis.

SUPPLEMENTARY DATA

Supplementary data are available online at www.aob.oxfordjournals.org and consist of the following. Figure S1: comparison of mean cell wall thickness of adjoining bundle sheath and mesophyll walls in three C_4 Sesuvioideae species. Figure S2: transmission electron micrographs of leaf blade cross-sections showing numerous plasmodesmata traversing adjoining mesophyll and bundle sheath walls in primary pit fields. Figure S3: light micrographs of *in situ* immunolocalizations of PEP-CK in cross-sections through leaves of comparison C_4 species.

ACKNOWLEDGMENTS

This research was funded by a research grant number 2/2009 to R.M. from the Deanship of Scientific Research and Graduate Studies of Yarmouk University. The authors thank Dr Nancy G. Dengler for review and assistance, Dr Norbert Kilian for providing *T. sheilae* seeds, Zakariya Bani Domi, Noor Al-Bo'ul, Mai Al-Shreideh, Ismail Zayed and Adel Rabab'ah for technical assistance, and the transmission electron microscope unit of Yarmouk University for use of the TEM facilities and for staff assistance.

LITERATURE CITED

Burnell JN, Hatch MD. 1988. Photosynthesis in phospho*enol*pyruvate carboxykinase-type C_4 plants: pathways of C_4 acid decarboxylation in bundle sheath cells of *Urochloa panicoides*. *Archives of Biochemistry and Biophysics* **260**: 187–199.

Carnal NW, Agostino A, Hatch MD. 1993. Photosynthesis in phospho*enol*-pyruvate carboxykinase-type C_4 plants: mechanism and regulation of C_4 acid decarboxylation in bundle sheath cells. *Archives of Biochemistry and Biophysics* **306**: 360–367.

Carolin RC, Jacobs SWL, Vesk M. 1978. *Kranz* cells and mesophyll in the Chenopodiales. *Australian Journal of Botany* **26**: 683–698.

Chen ZH, Walker RP, Acheson RM, Leegood RC. 2002. Phospho*enol*pyruvate carboxykinase assayed at physiological concentrations of metal ions has a high affinity for CO_2. *Plant Physiology* **128**: 160–164.

Dengler NG, Dengler RE, Donnelly PM, Filosa MF. 1995. Expression of the C_4 pattern of photosynthetic enzyme accumulation during leaf development in the C_4 dicot, *Atriplex rosea*. *American Journal of Botany* **82**: 318–328.

Dengler NG, Nelson T. 1999. Leaf structure and development in C_4 plants. In: Sage RF, Monson RK. eds. *C_4 plant biology*. San Diego: Academic Press, 133–172.

Edwards GE, Voznesenskaya EV. 2011. C_4 photosynthesis: Kranz forms and single-cell C_4 in terrestrial plants. In: Raghavendra AS, Sage RF. eds. *C_4 photosynthesis and related CO_2 concentrating mechanisms*. Dordrecht: Springer, 29–61.

Edwards GE, Walker DA. 1983. *C_3, C_4: mechanisms, and cellular and environmental regulation of photosynthesis*. Oxford: Blackwell Scientific.

Edwards G, Franceschi VR, Ku MSB, Voznesenskaya EV, Pyankov VI, Andreo CS. 2001. Compartmentation of photosynthesis in cells and tissues of C_4 plants. *Journal of Experimental Botany* **52**: 577–590.

Furbank RT. 2011. Evolution of the C_4 photosynthetic mechanism: are there really three C_4 acid decarboxylation types? *Journal of Experimental Botany* **62**: 3103–3108.

Gowik U, Westhoff P. 2011. The path from C_3 to C_4 photosynthesis. *Plant Physiology* **155**: 56–63.

Gutierrez M, Gracen VE, Edwards GE. 1974. Biochemical and cytological relationships in C_4 plants. *Planta* **119**: 279–300.

Hartmann HEK. 2001*a*. *Illustrated handbook of succulent plants: Aizoaceae A–E*. Berlin: Springer.

Hartmann HEK. 2001*b*. *Illustrated handbook of succulent plants: Aizoaceae F–Z*. Berlin: Springer.

Hartmann HEK, Meve U, Liede-Schumann S. 2011. Towards a revision of *Trianthema*, the Cinderella of Aizoaceae. *Plant Ecology and Evolution* **144**: 177–213.

Hassan NS, Thiede L, Liede-Schumann S. 2005. Phylogenetic analysis of Sesuvioideae (Aizoaceae) inferred from nrDNA internal transcribed spacer (ITS) sequences and morphological data. *Plant Systematics and Evolution* **255**: 121–143.

Hatch MD. 1987. C_4 photosynthesis: a unique blend of modified biochemistry, anatomy and ultrastructure. *Biochimica et Biophysica Acta* **895**: 81–106.

Hatch MD, Kagawa T. 1974. Activity, location, and role of NAD malic enzyme in leaves with C_4-pathway photosynthesis. *Australian Journal of Plant Physiology* **1**: 357–369.

Hatch MD, Kagawa T, Craig S. 1975. Subdivision of C_4 pathway species based on differing C_4 acid decarboxylating systems and ultrastructural features. *Australian Journal of Plant Physiology* **2**: 111–128.

Hatch MD, Tsuzuki M, Edwards GE. 1982. Determination of NAD malic enzyme in leaves of C_4 plants. Effects of malate dehydrogenase and other factors. *Plant Physiology* **69**: 483–491.

Heldt HW, Piechulla B. 2011. *Plant biochemistry*, 4th edn. Maryland: Elsevier Academic Press.

Kanai R, Edwards G. 1999. The biochemistry of C_4 photosynthesis. In: Sage RF, Monson RK. eds. *C_4 plant biology*. San Diego: Academic Press, 49–87.

Khoshravesh R, Akhani H, Sage TL, Nordenstam B, Sage RF. 2012. Phylogeny and photosynthetic pathway distribution in *Anticharis* Endl. (Scrophulariaceae). *Journal of Experimental Botany* **63**: 5645–5658.

Klak C, Khunou A, Reeves G, Hedderson T. 2003. A phylogenetic hypothesis for the Aizoaceae (Caryophyllales) based on four plastid DNA regions. *American Journal of Botany* **90**: 1433–1445.

Ku MSB, Monson RK, Littlejohn RO, Nakamoto H, Fisher DB, Edwards GE. 1983. Photosynthetic characteristics of C_3–C_4 intermediate *Flaveria* species. I. Leaf anatomy, photosynthetic responses to O_2 and CO_2, and activities of key enzymes in the C_3 and C_4 pathways. *Plant Physiology* **71**: 944–948.

Ku MSB, Wu J, Dai Z, Scott RA, Chu C, Edwards GE. 1991. Photosynthetic and photorespiratory characteristics of *Flaveria* species. *Plant Physiology* **96**: 518–528.

Lara MV, Drincovich MF, Andreo CS. 2004. Induction of a Crassulacean acid-like metabolism in the C_4 succulent plant, *Portulaca oleracea* L.: study of enzymes involved in carbon fixation and carbohydrate metabolism. *Plant and Cell Physiology* **45**: 618–626.

Marshall DM, Muhaidat R, Brown NJ, *et al*. 2007. *Cleome*, a genus closely related to *Arabidopsis*, contains species spanning a developmental progression from C_3 to C_4 photosynthesis. *The Plant Journal* **51**: 886–896.

McKown AD, Dengler NG. 2007. Key innovations in the evolution of Kranz anatomy and C_4 vein pattern in *Flaveria* (Asteraceae). *American Journal of Botany* **94**: 382–399.

Muhaidat R, Sage RF, Dengler NG. 2007. Diversity of *Kranz* anatomy and biochemistry in C_4 eudicots. *American Journal of Botany* **94**: 362–381.

Muhaidat R, Sage TL, Frohlich MW, Dengler NG, Sage RF. 2011. Characterization of C_3–C_4 intermediate species in the genus *Heliotropium* L. (Boraginaceae): Anatomy, ultrastructure and enzyme activity. *Plant, Cell and Environment* **34**: 1723–1736.

Muhaidat R, McKown AD, Al Khateeb W, *et al*. 2012. Full assessment of C_4 photosynthesis in *Blepharis attenuata* Napper (Acanthaceae) from Jordan: evidence from leaf anatomy and key C_4 photosynthetic enzymes. *Asian Journal of Plant Sciences* **11**: 206–216.

Parry MAG, Madgwick PJ, Carvalho JFC, Andralojc PJ. 2007. Prospects for increasing photosynthesis by overcoming limitations of Rubisco. *Journal of Agricultural Science* **145**: 31–43.

Prendergast HDV, Hattersley PW, Stone NE. 1987. New structural–biochemical associations in leaf blades of C_4 grasses (Poaceae). *Australian Journal of Plant Physiology* **14**: 403–420.

Reiskind JB, Bowes DG. 1991. The role of phospho*enol*pyruvate carboxykinase in a marine macroalga with C_4-like photosynthetic characteristics. *Proceedings of the National Academy of Sciences, USA* **88**: 2883–2887.

Reynolds ES. 1963. The use of lead citrate at high pH as an electron-opaque stain in electron microscopy. *Journal of Cell Biology* **17**: 208–212.

Sage RF. 2002. Variation in the k_{cat} of Rubisco in C_3 and C_4 plants and some implications for photosynthetic performance at high and low temperature. *Journal of Experimental Botany* **53**: 609–620.

Sage RF. 2004. The evolution of C_4 photosynthesis. *New Phytologist* **161**: 341–370.

Sage RF, Christin PA, Edwards EJ. 2011. The C_4 plant lineages of planet Earth. *Journal of Experimental Botany* **62**: 3155–3169.

Sharkey TD, Savitch LV, Butz ND. 1991. Photometric method for routine determination of k_{cat} and carbamylation of Rubisco. *Photosynthesis Research* **28**: 41–48.

Sommer M, Bräutigam A, Weber APM. 2012. The dicotyledonous NAD malic enzyme C_4 plant *Cleome gynandra* displays age-dependent plasticity of C_4 decarboxylation biochemistry. *Plant Biology* **14**: 621–629.

Spurr AR. 1969. A low-viscosity epoxy resin embedding medium for electron microscopy. *Journal of Ultrastructural Research* **26**: 31–43.

Sudderth EA, Muhaidat RM, McKown AD, Kocacinar F, Sage RF. 2007. Leaf anatomy, gas exchange and photosynthetic enzyme activity in *Flaveria kochiana*. *Functional Plant Biology* **34**: 118–129.

Takabayashi A, Kishine M, Asada K, Endo T, Sato F. 2005. Differential use of two cyclic electron flows around photosystem I for driving CO_2-concentration mechanism in C_4 photosynthesis. *Proceedings of the National Academy of Sciences, USA* **102**: 16898–16903.

Ueno O. 1992. Immunogold localization of photosynthetic enzymes in leaves of *Aristida latifolia*, a unique C_4 grass with a double chlorenchymatous bundle sheath. *Physiologia Plantarum* **85**: 189–196.

Vozenesenskaya EV, Franceschi VR, Pyankov VI, Edwards GE. 1999. Anatomy, chloroplast structure and compartmentation of enzymes relative to photosynthetic mechanisms in leaves and cotyledons of species in the tribe *Salsoleae* (*Chenopodiaceae*). *Journal of Experimental Botany* **50**: 1779–1795.

Voznesenskaya EV, Franceschi VR, Chuong SDX, Edwards GE. 2006. Functional characterization of phospho*enol*pyruvate carboxykinase type C_4 leaf anatomy: immuno, cytochemical and ultrastructural analyses. *Annals of Botany* **98**: 77–91.

Voznesenskaya EV, Chuong SDX, Koteyeva NK, Franceschi VR, Freitag H, Edwards GE. 2007. Structural, biochemical, and physiological characterization of C_4 photosynthesis in species having two vastly different types of *Kranz* anatomy in genus *Suaeda* (Chenopodiaceae). *Plant Biology* **9**: 745–757.

Voznesenskaya EV, Akhani H, Koteyeva NK, *et al*. 2008. Structural, biochemical, and physiological characterization of photosynthesis in two C_4 subspecies of *Tecticornia indica* and the C_3 species *Tecticornia pergranulata* (Chenopodiaceae). *Journal of Experimental Botany* **59**: 1715–1734.

Voznesenskaya EV, Koteyeva NK, Edwards GE, Ocampo G. 2010. Revealing diversity in structural and biochemical forms of C_4 photosynthesis and a C_3–C_4 intermediate in genus *Portulaca* L. (Portulacaceae). *Journal of Experimental Botany* **61**: 3647–3662.

Walker RP, Acheson RM, Presti LI, Leegood RC. 1997. Phospho*enol* pyruvate carboxykinase in C_4 plants: its role and regulation. *Australian Journal of Plant Physiology* **24**: 459–468.

Walker RP, Chen Z-H, Acheson RM, Leegood RC. 2002. Effects of phosphorylation on phospho*enol*pyruvate carboxykinase from the C_4 plant, Guinea Grass. *Plant Physiology* **128**: 165–172.

Wang JL, Klessig DF, Berry GO. 1992. Regulation of C_4 gene expression in developing amaranth leaves. *The Plant Cell* **4**: 173–184.

Wingler A, Walker RP, Chen Z-H, Leegood RC. 1999. Phospho*enol* pyruvate carboxykinase is involved in the decarboxylation of aspartate in the bundle sheath of maize. *Plant Physiology* **120**: 539–545.

Wintermans JFGM, De Mots A. 1965. Spectrophotometric characteristics of chlorophylls and their pheophytins in ethanol. *Biochimica et Biophysica Acta* **109**: 448–453.

Yoshimura Y, Kubota F, Ueno O. 2004. Structural and biochemical bases of photorespiration in C_4 plants: quantification of organelles and glycine decarboxylase. *Planta* **220**: 307–317.